KSCE Journal of Civil Engineering
DOI 10.1007/s12205-024-0569-7

pISSN 1226-7988, eISSN 1976-3808
www.springer.com/12205

Structural Engineering

Time-varying Multivariate Linear Regression Modeling of Temperature-induced Bearing Displacements of A Single Tower Cable-Stayed Bridge

Shi-yang Xu[a], **Gao-xin Wang**[a], **and Xin Zhou**[b]

[a]*Dept. of Civil Engineering, China University of Mining and Technology, 2 Daxue Rd, Tongshan District, Xuzhou 221116, China*
[b]*Dept. of Southeast University, 2 Sipailou Rd, Xuanwu District, Nanjing 210096, China*

ARTICLE HISTORY

Received 27 March 2024
Revised 8 June 2024
Accepted 18 June 2024
Published Online 15 August 2024

KEYWORDS

Bearing displacement
Measurement point temperature
Gradient temperature
Nonlinear characteristics
Time-varying coefficient model

ABSTRACT

Based on the monitoring temperature field and bearing displacement data of a single-tower cable-stayed bridge, the changing trends of temperatures, temperature differences and displacements are analyzed, and then the correlations between bearing displacements and temperatures as well as temperature differences are analyzed in long-term and short-term periods; furthermore, a time-varying multivariate linear regression model for simulation of temperature-induced displacements is put forward, and the Kalman filtering technique is employed to achieve the accurate values of time-varying coefficients in this model; Finally, the modeling accuracy is verified and compared with the traditional multiple linear model. The results show that the temperature-induced displacements are not only affected by uniform temperature but also affected by gradient temperatures, which should be fully considered during time-varying multiple linear regression modeling; the correlations between bearing displacements and temperatures shows a good linear relationship over a long period of time (such as in several months), and shows obvious nonlinear relationship over a short period of time (such as in one day), indicating that the correlation in different time scales is different; the time-varying multiple linear regression model considering not only the influence of uniform temperature and gradient temperature but also the linear and nonlinear correlations demonstrates better modeling accuracy, with errors of only 0.77%, 2.35%, and 2.58% for daily, monthly, and quarterly data, respectively, and the simulated values of bearing displacements are very close to the measured values, with the root mean square errors of only 0.8479 and 0.7149, indicating that the proposed time-varying multiple linear regression model has a good simulation accuracy of bearing displacements.

1. Introduction

With the continuous expansion of bridge construction throughout the world, the scale of bridge construction has increased significantly. In recent years, there have been reports of bridge fracture and collapse accidents continuing to occur worldwide, which has been a cause of concern for bridge engineers and technical researchers. For example, in order to ensure the anti-slip safety of main cable in the main saddle of long-span suspension bridge, Wang et al. investigated the contact and slip behaviors of main cable of the long-span suspension bridge (Wang et al., 2022); Tran-Ngoc et al. pointed out that the Guadalquivir bridge is has come into operation for a long time, and proposed a novel approach to model updating for the Guadalquivir bridge based on the vibration measurements combined with a hybrid metaheuristic search algorithm (Tran-Ngoc et al., 2022); Qin et al. assessed the condition of a concrete-filled steel tube arch bridge using in-situ vibration measurements, finite element model updating and an improved artificial fish swarm algorithm (Qin et al., 2024).

Bridge bearings are important components to bear the loads of main girders, and bearing damage will directly affect the safety of bridge. Currently, there are many bridge inspection or monitoring

CORRESPONDENCE Gao-xin Wang civilgxwangg@hotmail.com Dept. of Civil Engineering, China University of Mining and Technology., 2 Daxue Rd, Tongshan District, Xuzhou 221116, China

technologies to detect bearing damage or other bridge damage such as acoustic emission monitoring (Xu et al., 2023), digital image monitoring (Wang et al., 2020), infrared monitoring (Zheng et al., 2022) and LVDT sensor monitoring (Bai et al., 2022). Acoustic emission monitoring is a passive non-destructive testing technique that can monitor the internal activity of materials in real time and continuously, with advantages such as insensitivity to geometric shape and strong adaptability, but it also faces some challenges such as environmental noise interference, complexity in signal interpretation, which is difficult to accurately detect bearing wear at complex bridge site; digital image monitoring is a nondestructive technique, but it is usually used for monitoring damage on the bearing surface and is susceptible to weather such as rain and fog; infrared monitoring has the advantages of non-contact, high sensitivity and strong resistance, but it has the disadvantage of being greatly affected by environment and also having a limited measurement range, which is actually difficult to use for bearing inspection. Hence, data-driven method based on the monitoring data of LVDT sensors combined with temperature data has been widely used to evaluate the bearing damage with the advantage of little interference of weather and noise.

With regard to the data-driven method, the monitoring bearing displacement by LVDT sensors refers to the relative change between bridge bearings and beams (Gong and Agrawal, 2016; Wang and Ye, 2018; Wu et al., 2020; Mei et al., 2021). Hence, extensive studies have been dedicated to simulating and predicting bearing displacements using monitoring data, focusing on establishing correlation models between temperatures and thermally-induced displacements using data-driven method (Wu et al., 2021). For example, Wu et al. proposed an early-warning method for bearing displacement of long-span bridges using a proposed time-varying temperature-displacement model, and the results show that the modeling and prediction errors of the time-varying model are smaller than that of the linear model (Wu et al., 2024; Wu et al., 2024); Wang et al. employed a multivariate linear regression method to formulate a correlation model between the chord temperature and bearing displacement in a steel truss bridge (Wang et al., 2016). These methods can establish a correlation analysis between temperature and bearing displacement and predict bearing displacement changes through temperature changes, but there are also some defects of these methods. One defect is that the temperature variables have a correlation with each other because the temperatures at different locations have similar seasonal changing trends, which results in the temperature variables in the model are not independent; the other defect is that the temperature differences or gradient temperatures are not treated as variables for consideration in the time-varying temperature-displacement model, but in some cases there are high temperature differences existing in bridge girders.

Furthermore, artificial neural networks are also used to model the temperature-induced displacements. For example, Zheng et al. proposed a modeling approach utilizing long short-term memory (LSTM) neural networks to capture the multivariate relationship between temperature and bearing displacement (Zheng et al., 2021); Asad et al. constructed an prediction model for long-term horizontal displacement under varying external environmental conditions to bearing the reliable assessment of bridge structures using artificial neural network and Bayesian optimization, and the analysis of the results concludes that the proposed method can generate an robust long-term horizontal displacement prediction model (Asad et al., 2023); Huang et al. proposes a spatial -temporal nonlinear modeling method for temperature and temperature-induced bearing displacement (TIBD) of long-span single-pier rigid frame bridge based on DCNN-LSTM network with elastic modulus fusion (Huang et al., 2024). However, with regard to the artificial neural networks, there are also some defects of these methods. One defect is the number of layers in a neural network is an important parameter that determines the depth and complexity of the model; as the number of layers increases, the model can extract more feature information, thereby improving the accuracy and generalization ability of the model; but if the number of layers is too many, there will be over-fitting problems in this method, resulting in bad fitting results of testing data; the other defect is the weight and bias in neural networks are constant values without change with time; if bearing damage occurs in the future, the values of weight and bias will maybe not appropriate for accurate simulation of displacement under the influence of bearing damage.

In general, current researches on the simulation of bearing displacement mostly considers the linear correlation between uniform temperature and bearing displacement, without considering the influence of gradient temperatures and the nonlinear characteristics of temperature displacement, resulting in low model accuracy, which may overlook the abnormal changes in bearing displacements (Hoult et al., 2010; Xia and Chen, 2013). Therefore, in order to improve modeling accuracy and lay the foundation for achieving accurate assessment of bearing damage, it is necessary to conduct a deep research on displacement modeling considering the influence of gradient temperatures and the nonlinear characteristics of temperature-induced displacements.

Hence, this study analyzed a single-tower cable-stayed bridge using the monitoring data of temperatures and bearing displacements, which undertakes a thorough research of modeling the correlation between girder temperatures and bearing displacements at different time scales of daily change and monthly change. In this research, a time-varying multiple linear regression model is built, which considers not only the influence of uniform temperature and gradient temperature but also the monthly-linear and daily-nonlinear characteristics, and Kalman filtering method is used to accurately calculate the time-varying coefficients of the model. Finally, the modeling accuracy is verified and compared with the traditional multiple linear model, and the results show that the time-varying multiple linear regression model considering not only the influence of uniform temperature and gradient temperature but also the linear and nonlinear correlations demonstrates better modeling accuracy.

2. Project Overview

A cable-stayed bridge is located at the estuary of the Yongjiang River in Ningbo, Zhejiang Province, China, as shown in Fig. 1. There are five spans of main girder, and the length of each span is (74.5 + 258 + 102 + 83 + 49.5) m. The entire bridge is designed with six lanes in both directions with a speed of 60 km/h. The main girder is a pre-stressed concrete structure with a width of 29.5 meters and a height of 2.4 meters. The standard cross-section of the main girder is a double-box single-chamber section in an inverted trapezoidal shape. The bridge tower is a reinforced concrete structure with a thin-walled hollow box-shaped section, standing at a height of 148.4 meters with 25 pairs of diagonal stay cables distributed on each side.

This cable-stayed bridge, characterized by a large span, high-load design value, and complex structural type, requires the installation of a health monitoring system to continuously monitor the operation status of bridge structures, as shown in Fig. 1. The monitoring points on the main girder are primarily situated at sections A to J. The left and right structural forms of the main beam are the same, so temperature sensors have been strategically positioned on the right side, with a total of 5 temperature-monitoring sections and 53 temperature sensors. Displacement sensors are strategically placed on the top of the bridge piers (namely P20, P22, and P25), symmetrically distributed on both sides.

It should be pointed out that WD-G-01 or WY-G-01 denotes the 1st temperature or displacement sensor located in section G, and the numbering method for the other temperature and displacement sensors is the same. The distribution of measurement points for the main bridge temperature and bearing displacement is shown in Fig. 1.

3. Analysis of the Relationship between Main Girder Temperature Field and Bearing Displacement

3.1 Analysis of Main Girder Temperature and Bearing Displacement Monitoring Data

Cable-stayed bridges are flexible structures with small axial curvature and uniform cross-sectional changes, and the gradient temperatures along the longitudinal direction of main girders can be ignored (Yarnold et al., 2015; Gao et al., 2021). In this study, temperature data is collected over six months (182 days) at

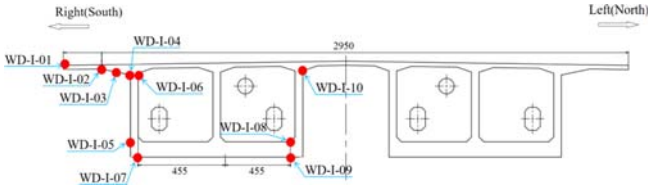

Fig. 2. Sensor Layout of Section I (Unit: cm)

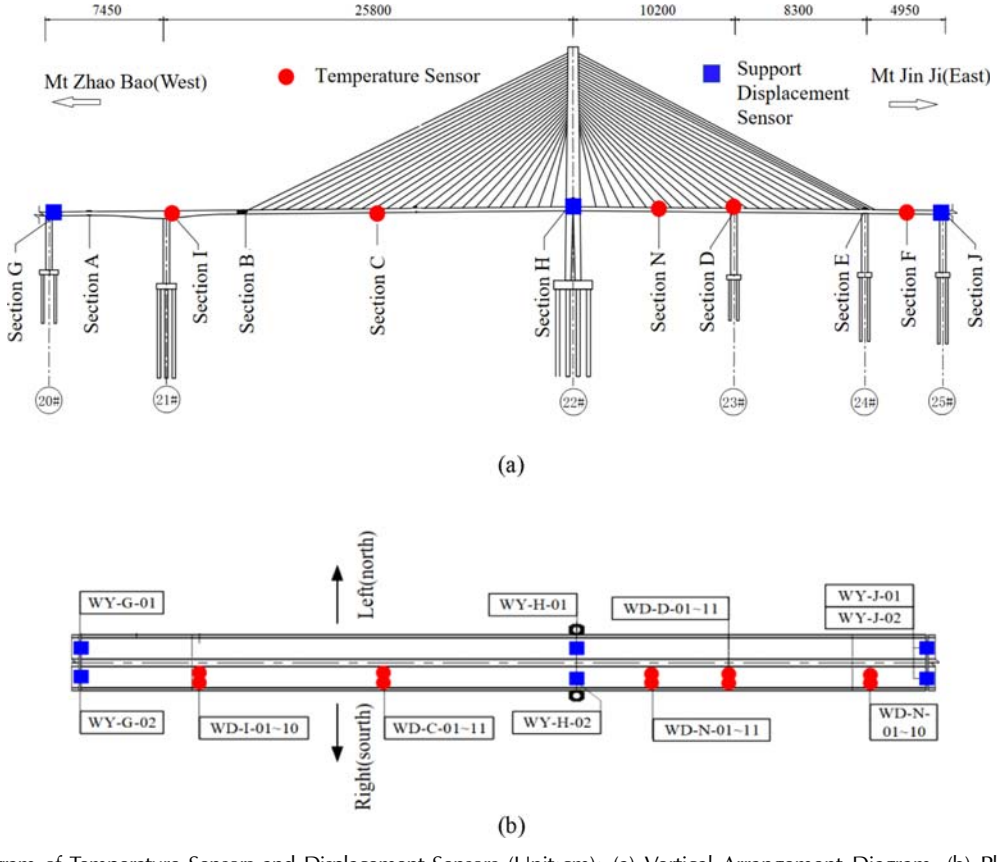

Fig. 1. Layout Diagram of Temperature Sensors and Displacement Sensors (Unit:cm): (a) Vertical Arrangement Diagram, (b) Planar Arrangement Diagram

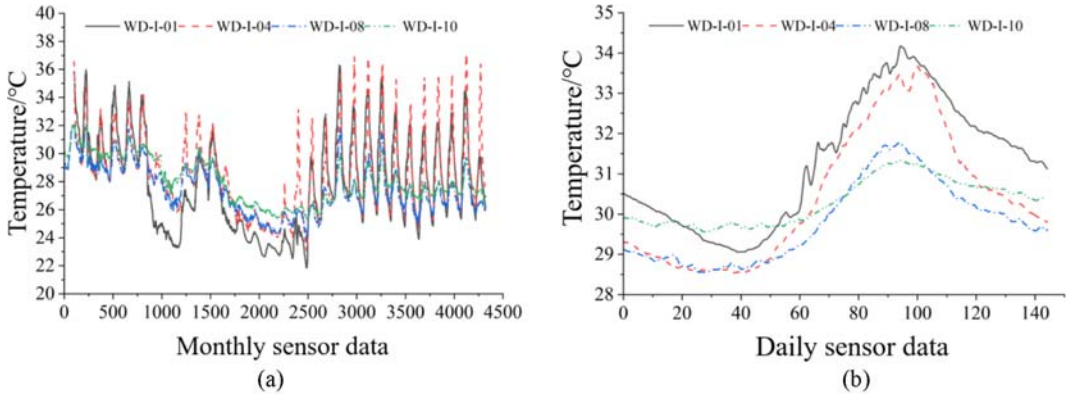

Fig. 3. Monthly anD Daily Temperature Variations for Measurement Points in Section I: (a) Monthly Variation, (b) Daily Variation

Section I for analysis, with the sensor layout illustrated in Fig. 2. The temperature data from the monitoring location WD-I-*i* is denoted by M_i, where i = 01, 02, ..., 10. The sampling frequency is set to 1 Hz.

The time histories of temperature data at different monitoring locations are shown in Fig. 3(a). It can be seen that the temperature ranges are different at different monitoring locations. For example, the temperature range of WD-I-01 is 21.9 – 37.9°C, and the temperature range of WD-I-10 is 25.2 – 32.1°C. In addition, the temperatures of different monitoring locations in the same day are also different, as shown in Fig. 3(b). For example, the temperature of WD-I-01 is 34.4°C at 14:30, and the temperature of WD-I-10 is 31.0°C at 14:30.

Furthermore, the values of temperature differences in section I of the main beam are calculated as shown in Table 1, where $T_{i,j}$ denotes the temperature differences between WD-I-*i* and WD-I-*j*. It can be seen that there is a significant gradient temperature in the vertical and transversal directions of the main beam section, with a maximum value of 18.7°C. This indicates that the temperature-induced displacements are not only affected by uniform temperature but also affected by gradient temperature, which should be carefully considered during time-varying multiple linear regression modeling.

Table 1. Statistical Values of Temperature Differences of Main Girder Section I

Lateral Temperature Differential Categories	Sensor Number	Max /°C	Min /°C
Horizontal Temperature Differential	I-$T_{1,4}$	13.2	-7.6
	I-$T_{6,10}$	4.7	-2.9
	I-$T_{5,9}$	4.2	-2.2
Vertical Temperature Differential	I-$T_{1,5}$	18.7	-7.6
	I-$T_{5,4}$	4.3	-2.5
	I-$T_{8,10}$	2.6	-2.2

The longitudinal displacements of the bearings on P20, P22 and P25 are measured using LVDT sensors. Consider that the bearings on P22 are constrained in the both longitudinal and transversal directions which results in very small displacement values, so this study primarily focuses on the analysis of bearing displacements on P20 and P25. The layout of displacement sensors on P20 is depicted in Fig. 4. The sampling frequency is set to 1 Hz.

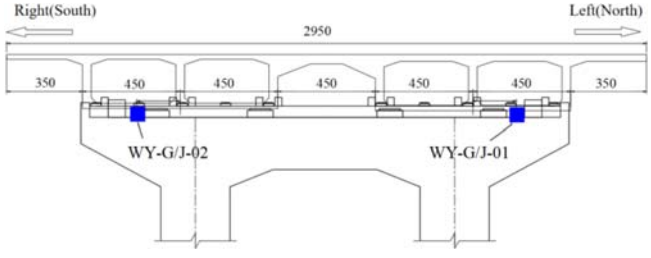

Fig. 4. Layout Diagram of Bearing Displacement Sensors

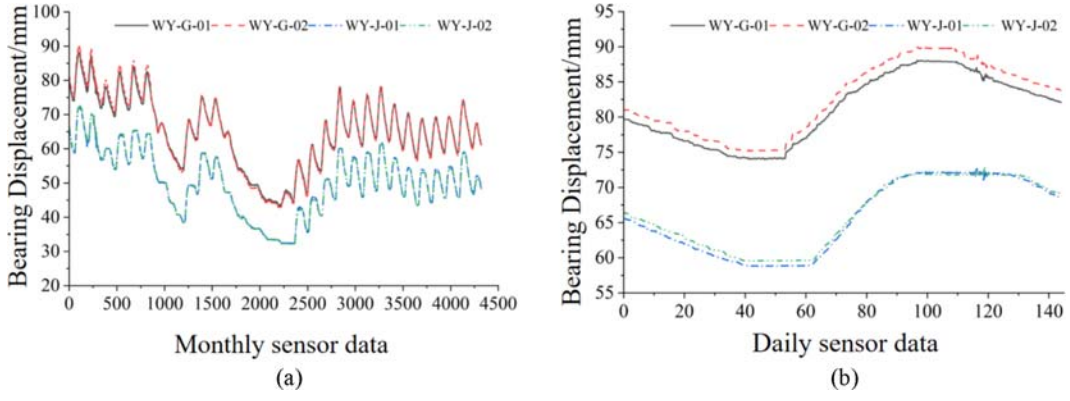

Fig. 5. Monthly and Daily Variations of Bearing Displacements: (a) Monthly Variation, (b) Daily Variation

The monthly and daily monitoring results of longitudinal displacements of the bearings on P20 (corresponding to WY-G-01/02) and P25 (corresponding to WY-J-01/02) are shown in Fig. 5. It can be seen that the whole trends of longitudinal displacements are similar, and especially the whole trends of longitudinal displacements of the same pier are very close such as WY-G-01 and WY-G-02, so the average values of the displacements are utilized to represent the bearing displacement of the same pier in the following study. In addition, the daily variation of bearing displacements follows a sinusoidal pattern. By comparison of the monitoring results from P20 and P25, the displacements of WY-G-01/02 are bigger than the displacements of WY-J-01/02, and the reason is that the girder span on the east side (corresponding to WY-G-01/02) of bridge tower is longer than the west side (corresponding to WY-J-01/02) of bridge tower, and the maximum displacement value is 89.93 mm from WY-G-02.

3.2 The Correlation Analysis between Main Girder Temperature Measurement Points and Bearing Displacement

By comparison of the trends of bearing displacements and temperatures, it can be found that they are similar, so it can be inferred that bearing displacements have correlation with temperatures, which is depicted in Fig. 6. It can be seen that there is a distinct positive linear correlation between bearing displacement and main girder temperature, indicating that bearing displacement will increase as temperature increases. This relationship can be expressed by a linear function $D = kT + b$ (where D represents

Table 2. Correlation Parameters between Temperatures and Displacements

Number	Temperature Sensor Number	Fitting Coefficients		R
		k	b	
1	WD-I-01	0.25	11.95	0.865
2	WD-I-02	0.24	11.97	0.867
3	WD-I-03	0.24	13.54	0.967
4	WD-I-04	0.23	14.31	0.855
5	WD-I-05	0.24	13.92	0.979
6	WD-I-06	0.22	13.79	0.964
7	WD-I-07	0.24	15.43	0.925
8	WD-I-08	0.21	13.79	0.963
9	WD-I-09	0.21	15.48	0.878
10	WD-I-10	0.20	14.95	0.943

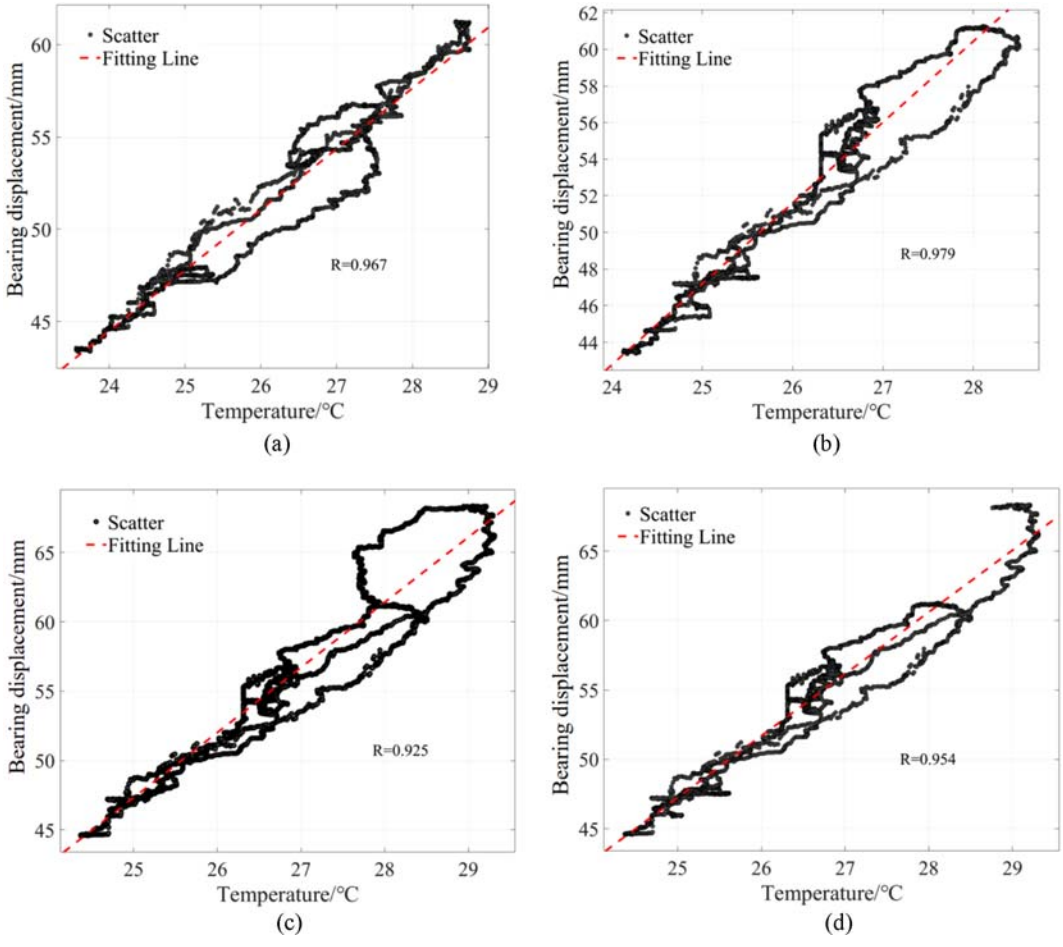

Fig. 6. Correlation between Temperatures and Displacements: (a) WD-I-03 and WY-G, (b) WD-I-05 and WY-G, (c) WD-I-07 and WY-J, (d) WD-I-10 and WY-J

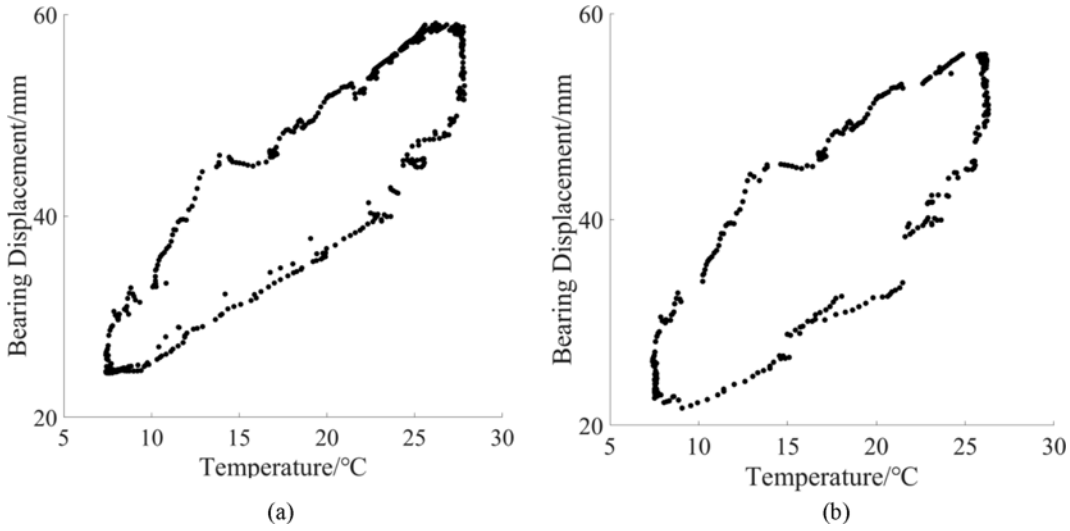

Fig. 7. Daily Correlation between Temperatures and Displacements: (a) WD-I-03 and WY-G, (b) WD-I-05 and WY-J

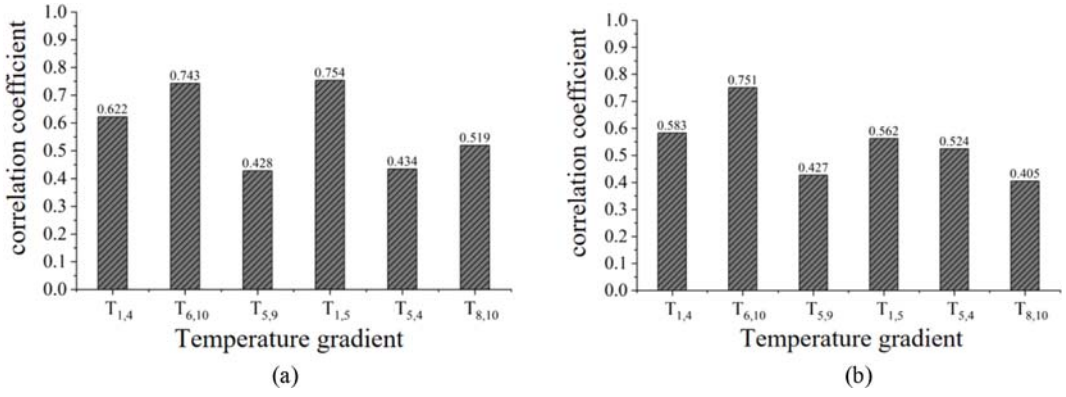

Fig. 8. Correlation between Temperature Gradients and Displacements: (a) Ds-G, (b) Ds-J

bearing displacement, T represents main girder temperature, and k, b are fitting parameters). Taking the bearing displacement WY-G-01 as an example, the values of fitting parameters are calculated using the least squares method, as shown in Table 2. The results indicate that the correlation coefficients between bearing displacement and main girder temperature are all greater than 0.85, verifying a robust linear correlation.

Furthermore, the daily correlation between bearing displacement and main girder temperature is analyzed. Fig. 7 presents the scatter plot depicting the daily correlation. It can be seen that the daily correlation shows an elliptical nonlinear characteristic, and the primary reason is that the change in bearing displacement typically lags behind the change in main girder temperature, indicating a lag effect (Guo et al., 2015; Han et al., 2017). It can be concluded that the correlation in different time scales is different, showing obvious linear relationship as well as nonlinear relationship.

3.3 Correlation Analysis between Gradient Temperature of Main Beam and Bearing Displacement

The influence of uniform temperature on bearing displacement is significant, which can mask the influence of gradient temperature on bearing displacement (Xia et al., 2017). Hence, the residual displacement after eliminating the uniform temperature impact on bearing displacement is calculated, denoted as D_s-G-i or D_s-J-i for the ith sensor. The values of correlation coefficients between residual displacements and gradient temperatures is depicted in Fig. 8. It is evident that for some gradient temperatures such as $T_{6,10}$, a robust correlation exists between some gradient temperatures and residual displacements, with a maximum correlation coefficient of 0.754; for some gradient temperatures such as $T_{5,9}$, the influence of gradient temperatures on bearing displacements is relatively weak and can be disregarded. Therefore, during considering the effect of gradient temperatures on longitudinal displacements, this study only selects gradient temperatures with a correlation coefficient greater than 0.55. What should be mentioned is that, with regard to our study case, the correlation coefficients less than 0.55 have weak influence on the simulation accuracy of bearing displacements after many times of simulation tests, so 0.55 is used as a criterion for the selection of correlation coefficients.

Based on the monitoring data of residual displacements D_S as well as gradient temperatures $T_{1,4}$, $T_{6,10}$, $T_{1,5}$, two days of data (day 45 and day 46) were selected to build the multivariate linear correlation models, as shown in Fig. 9. A noticeable observation is that the values of correlation coefficients are different in two

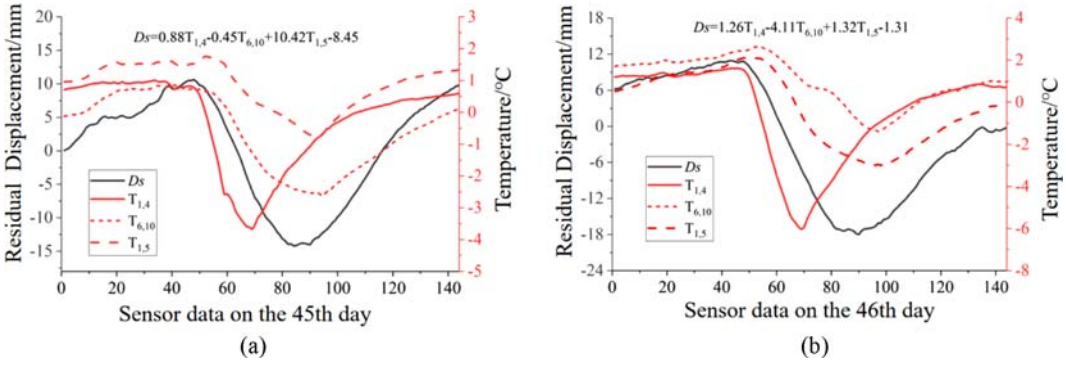

Fig. 9. Variation of Gradient Temperatures and Residual Displacements: (a) On the 45th Day, (b) On the 46th Day

days, indicating that the correlation coefficients are time-varying.

4. Time-Varying Model of Temperature and Bearing Displacement

4.1 Time-Varying Model Construction

Based on the above analysis, a robust linear relationship is identified between bearing displacement and both measurement point temperature and certain gradient temperatures. Furthermore, it is observed that the temperature coefficients show time-varying characteristics. Therefore, the correlation model between temperature variables and bearing displacement can be expressed as

$$D_j(t) = \xi_{1,j}(t)T_1(t) + \xi_{2,j}(t)T_2(t) + \cdots + \xi_{N,j}(t)T_N(t) + C_j\,. \tag{1}$$

$D_j(t)$ denotes the longitudinal displacement of the jth bearing, $\xi_{i,j}(t)$ denotes the jth time-varying coefficient, and $T_i(t)$ denotes the temperature variables including point temperatures and temperature gradients, and each point temperature and temperature gradient can be treated as a temperature variable, where i = 1, 2, ⋯, N, and C_j is a constant.

What should be mentioned is that the point temperatures $T_i(t)$ from different measurement points have similar trends and is not mutually independent, which is inappropriately treated as variables for modeling. Therefore, it is necessary to eliminate the correlation information from the original temperature variables. Hence, principal component analysis (PCA) is introduced (Wang et al., 2016). This method transforms multiple variables into principal components that retain the majority of the original information, and these components are mutually orthogonal. By extracting the principal components of the temperature variables $T_1(t), T_2(t), \cdots, T_N(t)$, denoted by $P_1(t), P_2(t), \cdots, P_Q(t)$, the expression of the multivariate linear regression model is improved as follows:

$$D_j(t) = \xi_{1,j}(t)P_1(t) + \xi_{2,j}(t)P_2(t) + \cdots + \xi_{Q,j}(t)P_Q(t) + C_j\,, \tag{2}$$

where $P_i(t)$ denotes the ith temperature principal component, Q denotes the number of temperature principal components, and C_j is a constant.

According to the contribution rates of the principal component, this paper extracts the top three principal components with contribution rates represented by PC1, PC2, and PC3. Their contribution rates are 92.49%, 4.59%, and 2.24%, respectively. The temperature principal component variation curves are illustrated in Fig. 10.

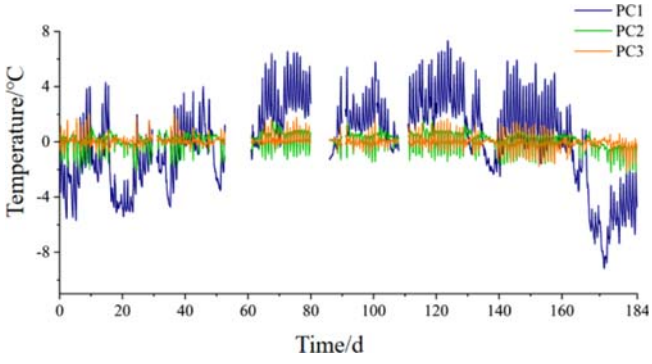

Fig. 10. Temperature Principal Components

4.2 Temperature Time-Varying Coefficient Solution

Kalman filtering is a time-domain recursive algorithm used for the solution of a state-space model (Chang et al., 2019). This method establishes a priori estimate $\hat{X}_{\bar{k}}$ based on the state at the previous moment, and subsequently determines the optimal estimate $\hat{X}_k$ by combining it with the observation value Z_k at the current moment. Through continuous "prediction-correction", the optimal estimation result is determined by incorporating observed data. The filter value can be updated in real-time as new observations become available. Many studies have proven that Kalman filtering has good performance in predicting the linear and nonlinear structural effects (Wang et al., 2013; Lyu et al., 2024; Song and Zheng, 2024), and Kalman filtering is widely used in bridge health monitoring. For example, Xiao et al. uses Kalman filtering to identify and quantify onboard data of track irregularities in vehicle vibration response (Xiao et al., 2022); Lee and Yun, proposed a sequential modified extended Kalman filtering algorithm that identifies unknown parameters and state vectors in two separate steps (Lee and Yun, 2008); Wu et al. proposed an Unscented Kalman Filter (UKF) method for identifying linear or nonlinear flutter derivatives of bridge decks from free vibration or vibrate

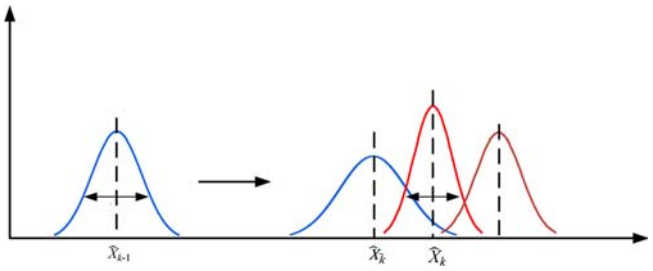

Fig. 11. Schematic Diagram of Kalman Filtering to Determine the Optimal Estimate $\hat{X}_k$

response time history (Wu et al., 2021).

The Kalman filtering method can accurately and effectively calculate the time-varying coefficients related to different temperature variables. Due to the fact that the time-varying coefficient is also a variable that constantly changes over time, the time-varying coefficient of linear or nonlinear correlation between temperature and displacement can be obtained ensuring the accuracy of the data. The principle of determining the optimal estimate in the Kalman filter is depicted in Fig. 11.

In light of the time-varying model for temperature-induced displacements, coupled with the Kalman filtering algorithm, the state equations proposed in this paper are as follows:

$$D_j(t) = \Psi_j(t)P(t) + C_j\,, \tag{3}$$

$$\Psi_j(t+1) = \Omega_j \Psi_j(t) + V_j(t)\,, \tag{4}$$

where $D_j(t)$ denotes the longitudinal displacement matrix, encompassing the monitoring data for longitudinal displacement; $P(t)$ denotes the temperature principal component matrix; $\Psi_j(t)$ denotes the time-varying coefficient matrix, $\Psi_j(t) = [\xi_{1,j}(t), \xi_{2,j}(t), \cdots, \xi_{Q,j}(t)]^T$; Ω_j denotes the iteration matrix, and $V_j(t)$ denotes the noise matrix.

The bearing damage can be identified by analyzing the abnormal correlation changes between temperature and bearing displacement (Webb and Middleton, 2013; Nord et al., 2015). Consequently, the time-varying coefficients are utilized for the preliminary identification of bearing damage. If the time-varying coefficients show a abnormal change, it indicates the occurrence of bearing damage; otherwise, the bearing is considered to be in a healthy state.For example, the time-varying coefficients between WY-G and PC1, PC2, and PC3 of the cable-stayed bridge are plotted in Fig. 12. It is shown that the time-varying coefficients $\xi_1(t)$, $\xi_2(t)$, and $\xi_3(t)$ initially change with wide fluctuation, and then gradually tend to flatten out. Specifically, the time-varying coefficient $\xi_1(t)$ varies from a minimum value of 30.49 to a maximum value of 31.52, the time-varying coefficient $\xi_2(t)$ varies from a minimum value of 31.84 to a maximum value of 32.50, and the time-varying coefficient $\xi_3(t)$ varies from a minimum value of 32.40 to a maximum value of 34.16, respectively. Based on the trend of the time-varying coefficients, it can be determined that the bearing of the cable-stayed bridge are in a healthy state.

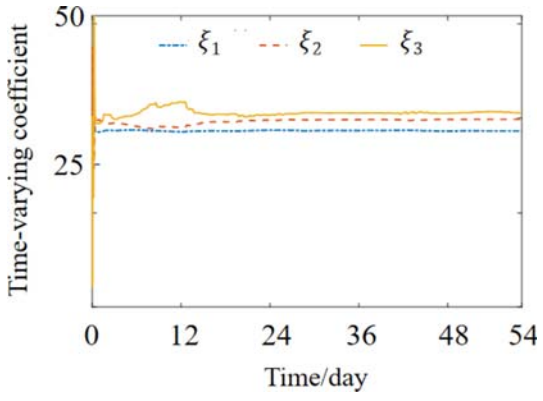

Fig. 12. Temperature Time-Varying Coefficients

4.3 Modeling Validation

The traditional multiple linear regression model is a widely-used method for simulating bearing displacements, and its structural form is presented in Eq. (5) as follows:

$$D_j(t) = \alpha_{1,j}T_1(t) + \alpha_{2,j}T_2(t) + \alpha_{3,j}T_3(t) + \cdots + \alpha_{N,j}t_N(t) + c_j\,. \tag{5}$$

Where $D_j(t)$ denotes the bearing displacement; $T_1 \sim T_N$ denotes the temperature variables; $\alpha_{1,j} \sim \alpha_{N,j}$ denotes the regression coefficients, which can be determined using the least squares method; and c_j is a constant term.

In this modeling validation, the simulation accuracy of the traditional model and the proposed time-varying model is compared. Daily, monthly, and quarterly monitoring data of displacements and temperatures are used for a comparative analysis of modeling accuracy. The modeling errors for the two models are calculated as follows:

$$E_{re} = \frac{D_{re,j}(t) - D_j(t)}{D_j(t)} \times 100\%\,, \tag{6}$$

$$E_{kf} = \frac{D_{kf,j}(t) - D_j(t)}{D_j(t)} \times 100\%\,, \tag{7}$$

where E_{re} and E_{kf} denote the modeling errors of traditional and time-varying methods, respectively; $D_{re,\,j}$ denotes the simulated values of bearing displacement obtained by traditional model; $D_{kf,j}$ denotes the simulated values of bearing displacement obtained by time-varying model.

The modeling errors for the two models, considering bearing displacements WY-G and WY-J, are shown in Fig. 13. It can be seen that for both WY-G and WY-J, the daily modeling error is maximally 2.51% for the multiple linear regression model and 0.77% for the time-varying model; the monthly modeling error is maximally 3.88% for the multiple linear regression model and 2.35% for the time-varying model; the quarterly modeling error is maximally 5.21% for the multiple linear regression model and 2.58% for the time-varying model. Hence, the time-varying model has higher modelling accuracy than multiple linear regression model.

Furthermore, the one-day time histories of the measured and

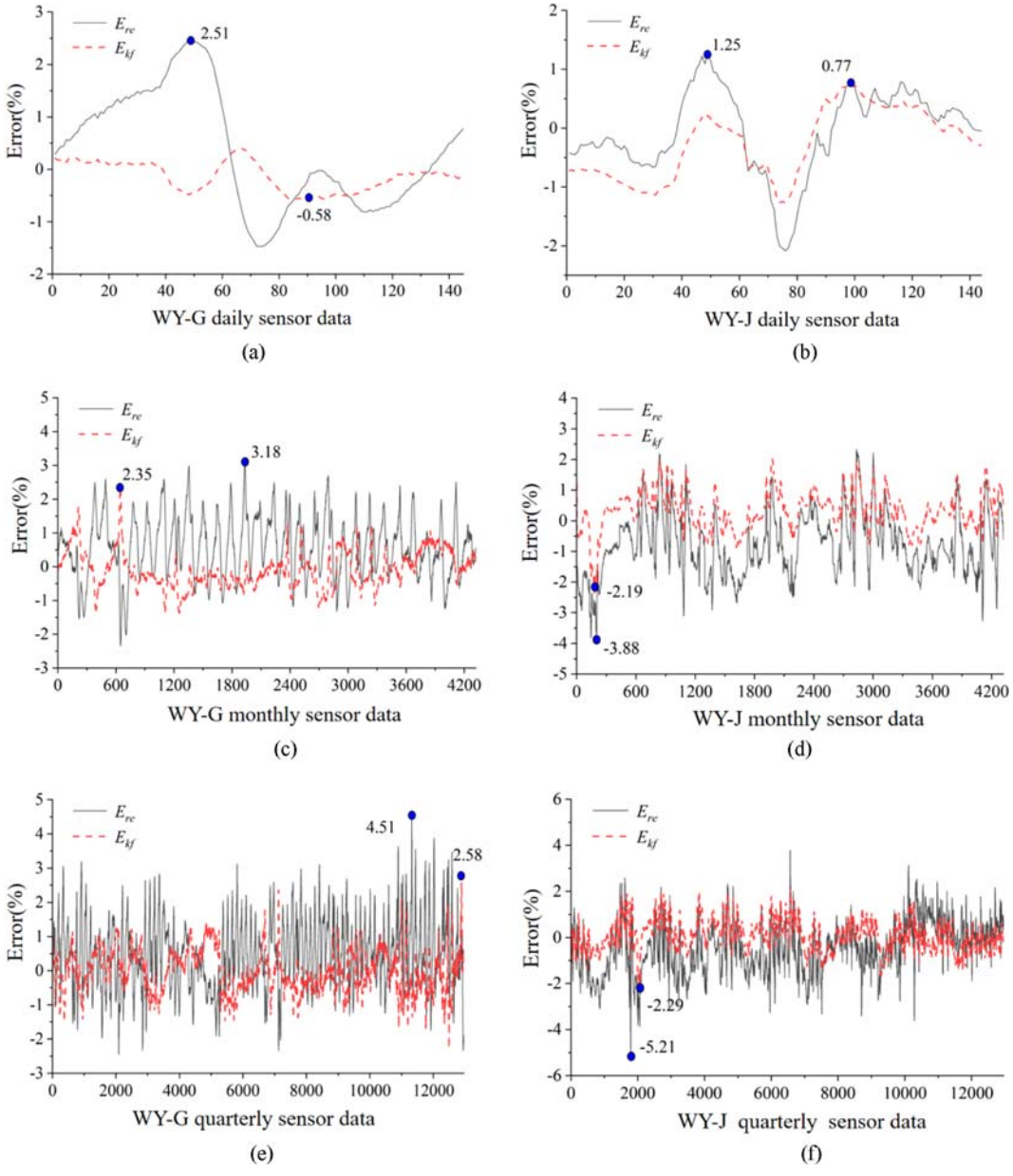

Fig. 13. Comparison of Modeling Simulation of Multiple Linear Regression Model and Time-Varying Model: (a) WY-G Daily Data, (b) WY-J Daily Data, (c) WY-G Monthly Data, (d) WY-J Monthly Data, (e) WY-G Quarterly Data, (f) WY-J Quarterly Data

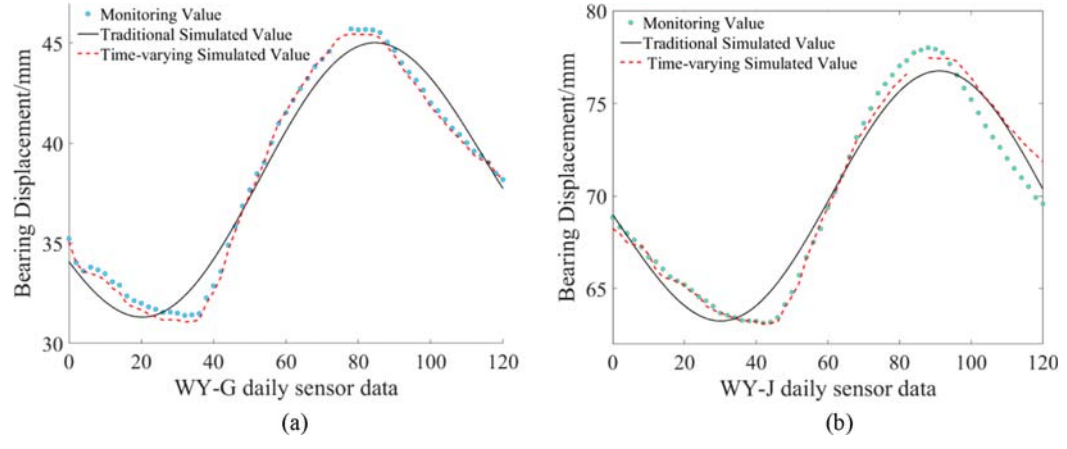

Fig. 14. Comparison of Measured and Predicted Bearing Displacements: (a) WY-G, (b) WY-J

simulated bearing displacements are shown in Fig. 14, where the simulated bearing displacements are obtained by two methods which are the traditional method (Eq. (5)) and the proposed time-varying method (Eq. (2)). It is evident that the simulated values calculated by the proposed time-varying method are closer to the measured values than the traditional method, with the root mean square errors of 0.8479 and 0.7149, respectively, verifying that the proposed time-varying multiple linear regression model has a good simulation accuracy of bearing displacements.

5. Conclusions

In order to improve the simulation accuracy of temperature-induced bearing displacements, this research puts forward a time-varying multiple linear regression modeling, which obtains better simulation accuracy by comparison with traditional simulation methods. The main conclusions are drawn as follows:

1. The monitoring temperature results show that there is a significant gradient temperature in the vertical and transversal directions of the main beam section, with a maximum value of 18.67°C. This indicates that the temperature-induced displacements are not only affected by uniform temperature but also affected by gradient temperature, which should be fully considered during time-varying multiple linear regression modeling;
2. The monthly correlation between displacement and uniform temperature or gradient temperature shows distinct positive linear characteristics; and the daily correlation shows an elliptical nonlinear characteristic, and the primary reason is that the change in bearing displacement typically lags behind the change in main girder temperature, indicating a lag effect. It can be concluded that the correlation in different time scales is different, showing obvious linear relationship in long-term period as well as nonlinear relationship in short-term period;
3. A time-varying multiple linear regression model is proposed which considers not only the influence of uniform temperature and gradient temperature but also the linear and nonlinear correlations; Kalman filtering method is used to accurately calculate the time-varying coefficients of the model; furthermore, the values of time-varying coefficients are feasible to evaluate the longitudinal expansion performance of bridge bearings;
4. Compared with traditional multivariate linear regression model, the time-varying multiple linear regression model considering long-term and short-term nonlinear relationship demonstrates better modeling accuracy, with errors of only 0.77%, 2.35%, and 2.58% for daily, monthly, and quarterly data, respectively; the simulated values of bearing displacements are close to the monitoring values, with the root mean square errors of only 0.8479 and 0.7149, suggesting that the time-varying multiple linear regression model has a good simulation accuracy of bearing displacements.

What should be mentioned is that, although this research object is a cable-stayed bridge with concrete box girder in this research, the proposed model can be applied to the other bridge types for high-accuracy displacement simulation, especially if the bridge girder contains obvious gradient temperature and the monthly correlation between displacement and temperature is nonlinear.

Acknowledgments

The authors gratefully acknowledge the the National Natural Science Foundation of China (grant number 51908545).

ORCID

Shi-yang Xu https://orcid.org/0009-0000-4877-7634
Gaoxin Wang https://orcid.org/0000-0001-8422-0120
Xin Zhou https://orcid.org/0009-0004-4805-0215

References

Asad AT, Kim B, Cho S, Sim SH (2023) Prediction model for long-term bridge bearing displacement using artificial neural network and bayesian optimization. *Structural Control and Health Monitoring* DOI: 10.1155/2023/6664981

Bai J, Diao Y, Jia C, etc (2022) A review of advances in triaxial tests: Instruments, test techniques and prospects. *KSCE Journal of Civil Engineering* 26(8):3325-3341, DOI: 10.1007/s12205-022-1345-1

Chang P, Wang YJ, Wu YF, Yang N (2019) Identification of temperature-sensitive structural damage based on principal component analysis. *Journal of Vibration Engineering* 32(2):7 (in Chinese)

Gao J, Lin JW, Wang BR (2021) Study of sunshine temperature effect on flat steel box girder based on measured data. *World Bridge* 49(4):69-76, DOI: 10.3969/j.issn.1671-7767.2021.04.011 (in Chinese)

Gong X, Agrawal AK (2016) Safety of cable-supported bridges during fire hazards. *Journal of Bridge Engineering* 21(4):1-12, DOI: 10.1061/(ASCE)BE.1943-5592.0000870

Guo T, Liu J, Zhang YF, Pan S (2015) Displacement monitoring and analysis of expansion joints of long-span steel bridges with viscous dampers. *Journal of Bridge Engineering* 20(9):1-11, DOI: 10.1061/(ASCE)BE.1943-5592.0000701

Han WC, Diao F, Zeng ZW (2017) Research on temperature effect of steel truss concrete T-structure composite bridge. *Northern Transportation* (6):6-10+16, DOI: 10.15996/j.cnki.bfjt.2017.06.002 (in Chinese)

Hoult NA, Fidler P, Hill PG, Middleton C (2010) Long-term wireless structural health monitoring of the ferriby road bridge. *Journal of Bridge Engineering* 15(2):153-159, DOI: 10.1061/(ASCE)BE.1943-5592.0000049

Huang M, Zhang J, Hu J, Ye Z, Deng Z, Wan N (2024) Nonlinear modeling of temperature-induced bearing displacement of long-span single-pier rigid frame bridge based on DCNN-LSTM. *Case Studies in Thermal Engineering* 53(103897), DOI: 10.1016/j.csite.2023.103897

Lee KJ, Yun CB (2008) Parameter identification for nonlinear behavior of RC bridge piers using sequential modified extended Kalman filter. *Smart Structures and Systems* 4(3):319-342, DOI: 10.12989/sss.2008.4.3.319

Lyu XX, Duan PH, Duan ZS, etc (2024) Stability analysis of constrained distributed nonlinear and linear kalman filters for dynamical systems

with state constraints. *IEEE Transactions on Aerospace and Electronic Systems* 60(1):632-643, DOI: 10.1109/TAES.2023.3328849

Mei DP, Zhou X, Wang G (2021) A fine simulation method for longitudinal displacement of bearing considering nonlinear time-varying correlation characteristics. *Bridge Construction* 51(5):7, DOI: 10.3969/j.issn.1003-4722.2021.05.011 (in Chinese)

Nord T, Lourens EM, Oiseth O, Metrikine A (2015) Model-based force and state estimation in experimental ice-induced vibrations by means of Kalman filtering. *Cold Regions Science & Technology* 111(3):13-26, DOI: 10.1016/j.coldregions.2014.12.003

Qin SQ, Feng JC, Tang J, etc (2024) Condition assessment of a concrete filled steel tube arch bridge using in-situ vibration measurements and an Improved Artificial Fish Swarm Algorithm. *Computers & Structures* 291(107213), DOI: 10.1016/j.compstruc.2023.107213

Song XM, Zheng WX (2024) A Kalman-filtering derivation of input and state estimation for linear discrete-time systems with direct feedthrough. *Automatica* 161(111453), DOI: 10.1016/j.automatica.2023.111453

Tran-Ngoc H, Khatir S, Le-Xuan T, etc (2022) Finite element model updating of a multispan bridge with a hybrid metaheuristic search algorithm using experimental data from wireless triaxial sensors. *Engineering with Computers* 38(Suppl 3):1865-1883, DOI: 10.1007/s00366-021-01307-9

Wang DP, Zhu HL, Xu W, etc (2022) Contact and slip behaviors of main cable of the long-span suspension bridge. *Engineering Failure Analysis* 136(106232), DOI: 10.1016/j.engfailanal.2022.106232

Wang GX, Ding YL, Song YS, Wu L, Yue Q, Mao G (2016) Detection and location of the degraded bearings based on monitoring the longitudinal expansion performance of the main girder of the dashengguan yangtze bridge. *Journal of Performance of Constructed Facilities* 30(4):04015074, DOI: 10.1061/(ASCE)CF.1943-5509.0000820

Wang GX, Ye JH (2018) Localization and quantification of partial cable damage in the long-span cable-stayed bridge using the abnormal variation of temperature-induced girder deflection. *Structural Control & Health Monitoring* 26(1):13-21, DOI: 10.1002/stc.2281

Wang J, Guo ZX, Zhang P, etc (2020) Fracture properties of rubberized concrete under different temperature and humidity conditions based on digital image correlation technique. *Journal of Cleaner Production,* 276, DOI: 10.1016/j.jclepro.2020.124106

Wang SY, Feng JC, Tse Ck (2013) Analysis of the characteristic of the kalman gain for 1-D chaotic maps in cubature kalman filter. *IEEE Signal Processing Letters* 20(3):229-232, DOI: 10.1109/LSP.2013.2241424

Webb GT, Middleton C (2013) Structural health monitoring of the hammersmith flyover. *IABSE Symposium Report* 99(27):152-153, DOI: 10.2749/222137813806474615

Wu GM, Li SL, Yi TH, Mei XD, Wang YF (2023) Theoretically thermal-varying models of the neutral axis position for local damage detection of bridge girders. *Engineering Structures* 279(1):115635, DOI: 10.1016/j.engstruct.2023.115635

Wu GM, Yi TH, Yang DH, etc (2021) Early warning method for bearing displacement of long-span bridges using a proposed time-varying temperature-displacement model. *Journal of Bridge Engineering* 26(9), DOI: 10.1061/(ASCE)BE.1943-5592.0001763

Wu GM, Zhang B, Li SL, Yi TH, Mei XD, Wang YF (2024) Neutral axis-based anomaly detection for local damage of girders with nonlinear temperature gradient. *Journal of Bridge Engineering-ASCE* 29(3):04024005, DOI: 10.1061/JBENF2.BEENG-6469

Wu LY, Liu XW, Zhao DC, Liu H, Chen B (2020) Calculation method of cumulative displacement of bridge bearings based on correlation statistical counting. *World Bridge* 48(5):6, DOI: 10.3969/j.issn.1671-7767.2020. 05.013 (in Chinese)

Wu YC, Chen XZ, Wang YF (2021) Identification of linear and nonlinear flutter derivatives of bridge decks by unscented Kalman filter approach from free vibration or stochastic buffeting response. *Journal of Wind Engineering and Industrial Aerodynamics* 214(104650), DOI: 10.1016/j.jweia.2021.104650

Xia Q, Zhang J, Tian YD, Zhang Y (2017) Experimental study of thermal effects on a long-span suspension bridge. *Journal of Bridge Engineering* 22(7):1-9, DOI: 10.1061/(ASCE)BE.1943-5592.0001083

Xia Y, Chen B (2013) Field monitoring and numerical analysis of tsing ma suspension bridge temperature behavior. *Structural Control & Health Monitoring* 20(4):560-575, DOI: 10.1002/stc.515

Xiao X, Xu XY, Shen WA (2022) Identification of frequencies and track irregularities of railway bridges using vehicle responses: A recursive bayesian kalman filter algorithm. *Journal of Engineering Mechanics* 148(9):04022051, DOI: 10.1061/(ASCE)EM.1943-7889.0002140

Xu J, Chang FJ, Bai JT, Liu CY (2023) Statistical analysis on the fracture behavior of rubberized steel fiber reinforced recycled aggregate concrete based on acoustic emission. *Journal of Materials Research and Technology* 24:8997-9014, DOI: 10.1016/j.jmrt.2023.05.124

Yarnold MT, Moo FL, Aktan AE (2015) Temperature-based structural identification of long-span bridges. *Journal of Structural Engineering,* 04015027, DOI: 10.1061/(ASCE)ST.1943-541X.0001270

Zheng QY, Zhou GD, Liu DK (2021) Temperature-displacement correlation modeling method for large-span arch bridges based on long and short-term memory neural networks. *Engineering Mechanics* 38(4):68-79, DOI: 10.6052/j.issn.1000-4750.2020.05.0323 (in Chinese)

Zheng YX, Wang SQ, Zhang P, etc (2022) Application of nondestructive testing technology in quality evaluation of plain concrete and RC structures in bridge engineering: A review. *Buildings* 12(6):843, DOI: 10.3390/buildings12060843